



Detection of radiation-exposure biomarkers by differential mobility prefiltered mass spectrometry (DMS–MS)

Stephen L. Coy^{a,*}, Evgeny V. Krylov^a, Bradley B. Schneider^b, Thomas R. Covey^b, David J. Brenner^c, John B. Tyburski^d, Andrew D. Patterson^d, Kris W. Krausz^d, Albert J. Fornace^e, Erkinjon G. Nazarov^a

^a *Sionex Corporation, 8-A Preston Ct., Bedford, MA 01730, United States*

^b *AB SCIEX, 71 Four Valley Drive, Concord, Ontario, L4K 4V8, Canada*

^c *Center for Radiological Research, Columbia University, New York, NY 10032, United States*

^d *Laboratory of Metabolism, Center for Cancer Research, National Cancer Institute, Bethesda, MD 20892, United States*

^e *Lombardi Comprehensive Cancer Center and Dept. of Biochemistry and Molecular & Cellular Biology, Georgetown University, Washington, DC 20057, United States*

ARTICLE INFO

Article history:

Received 15 October 2009

Received in revised form 11 January 2010

Accepted 19 January 2010

Available online 28 January 2010

Keywords:

Metabolomic

Radiation exposure

DMS

Ion mobility

Electrospray

ABSTRACT

Technology to enable rapid screening for radiation exposure has been identified as an important need, and, as a part of a NIH/NIAD effort in this direction, metabolomic biomarkers for radiation exposure have been identified in a recent series of papers. To reduce the time necessary to detect and measure these biomarkers, differential mobility spectrometry–mass spectrometry (DMS–MS) systems have been developed and tested. Differential mobility ion filters preselect specific ions and also suppress chemical noise created in typical atmospheric-pressure ionization sources (ESI, MALDI, and others). Differential-mobility-based ion selection is based on the field dependence of ion mobility, which, in turn, depends on ion characteristics that include conformation, charge distribution, molecular polarizability, and other properties, and on the transport gas composition which can be modified to enhance resolution. DMS–MS is able to resolve small-molecule biomarkers from isobaric interferences, and suppresses chemical noise generated in the ion source and in the mass spectrometer, improving selectivity and quantitative accuracy. Our planar DMS design is rapid, operating in a few milliseconds, and analyzes ions before fragmentation. Depending on MS inlet conditions, DMS-selected ions can be dissociated in the MS inlet expansion, before mass analysis, providing a capability similar to MS/MS with simpler instrumentation. This report presents selected DMS–MS experimental results, including resolution of complex test mixtures of isobaric compounds, separation of charge states, separation of isobaric biomarkers (citrate and isocitrate), and separation of nearly isobaric biomarker anions in direct analysis of a bio-fluid sample from the radiation-treated group of a mouse-model study. These uses of DMS combined with moderate resolution MS instrumentation indicate the feasibility of field-deployable instrumentation for biomarker evaluation.

© 2010 Elsevier B.V. All rights reserved.

1. Introduction

Discovery of small molecule biomarkers for radiation exposure by means of metabolomic studies is the subject of an extensive on-going investigation by an international team of investigators working at the National Cancer Institute (NCI/NIH), Georgetown University and the University of Bern, and overseen by the Center for High-Throughput Minimally-Invasive Radiation Biodosimetry at Columbia University (<http://cmcr.columbia.edu/>). The current published results [1–4] identify a number of validated and potential small molecule urinary metabolites that are associated with

sub-lethal radiation exposure in mouse models and are potentially useful in human screening. The initial paper in that group [1] includes a historical overview and a discussion of the sources and impact of radiation exposure. Development of rapid, field-deployable radiation-exposure screening methods is a priority area of research [5] because of the public health danger of the intentional or accidental release of radioactive material [6], and limitations of current radiation biodosimetry techniques.

The use of metabolomics for the discovery of biomarkers for radiation exposure is one of the more promising new approaches to radiation biodosimetry, but field-deployable instrumentation with sufficient speed, selectivity and quantitative accuracy is not yet available. To reduce the time necessary to detect and measure these biomarkers, differential mobility spectrometry–mass spectrometry (DMS–MS) systems have been developed and tested.

* Corresponding author. Tel.: +1 781 457 5377; fax: +1 781 457 5399.
E-mail address: scoy@sionex.com (S.L. Coy).

The use of differential mobility ion filters for mass spectrometry has a long history, dating to 1993 [7–10], and, as a result, several acronyms are used for devices based on the difference between high and low field ion-mobility coefficients. The term FAIMS (field-asymmetric ion-mobility spectrometry) is in common use, especially for electrodes in a cylindrical configuration, while DMS, or PFAIMS (planar FAIMS) are terms often used for the planar configuration. Applications and instrumentation have evolved considerably in the years since the earliest studies, and recent work has been validating 2D DMS–MS as an analytical technique [11–16]. DMS ion pre-filtration selects specific ions based on properties such as conformation, charge distribution, molecular polarizability, and others that cause the mobility coefficient for an ion in a neutral gas or gas mixture to be different in high field than in low field. Because these properties are largely orthogonal to m/z , two-dimensional combinations of DMS with mass spectrometry can be more selective than either instrument separately, and, because DMS can operate on the molecular ion prior to fragmentation, DMS–MS can be significantly more sensitive than MS/MS. Planar DMS separation operates in a few ms and has potential to eliminate mass spectral interferences regardless of their origin. As noted in the discussion of biomarker discovery methods in Lanz et al. [3], it is often the case that “[a]n unknown proportion of these ions arises from in-source fragmentation, adducts, dimers, and isotopes.” DMS is able to suppress this type of interference, greatly improving quantitative accuracy, potentially eliminating the need for alternate noise suppression approaches such as high resolution and multiple stages of mass spectrometry.

Because the DMS ion filter is generally operated at atmospheric pressure, DMS can be used in combination with other separation techniques such as GC [17,18] and LC [10], and with any atmospheric pressure ionization (API) source, including ESI, MALDI, radioactive sources, UV [19], discharge, and others [13]. In addition, DMS-filtered ions can be detected by any appropriate detector including mass spectrometry, electrometer detection, surface-enhanced Raman [20], and other techniques. The radiation-exposure biomarker discovery work has so far made use of time-of-flight mass spectrometry (TOFMS) in combination with high-resolution ultra-performance liquid chromatography (UPLC) [1,2,4], and capillary gas chromatography combined with mass spectrometry (GC–MS) following derivatization [3], but these techniques are costly and are too time-consuming for rapid screening applications. The use of a fast and effective separation technique like DMS API ion filtration can reduce the time necessary for the LC or GC steps, and allow use of simplified mass spectrometer technology.

This report presents selected DMS–MS experimental results, including resolution of test mixtures of isobaric compounds, separation of charge states, separation of isobaric biomarkers (citrate and isocitrate), and DMS–MS performance in direct analysis of a bio-fluid sample from the radiation-treated group of a mouse-model study. Our results show that planar differential mobility ion filters is a powerful addition to mass spectrometric methods for biomarker detection.

2. Experimental methods

Planar differential mobility interfaces were constructed for single quadrupole (Waters ZQ) and for time-of-flight instruments (JEOL Accutof), following the design shown in Fig. 1. Gas loads for the two instruments are $600\text{ cm}^3/\text{min}$ and $1000\text{ cm}^3/\text{min}$, respectively. The microspray ion source uses a Proxeon stainless steel emitter (ES561) connected to a syringe pump (Harvard Apparatus) using Valco micro-volume fittings. Ions from the electrospray plume enter a desolvation region preceding the DMS ion filter that is supplied with heated nitrogen gas. In this system, DMS and mass

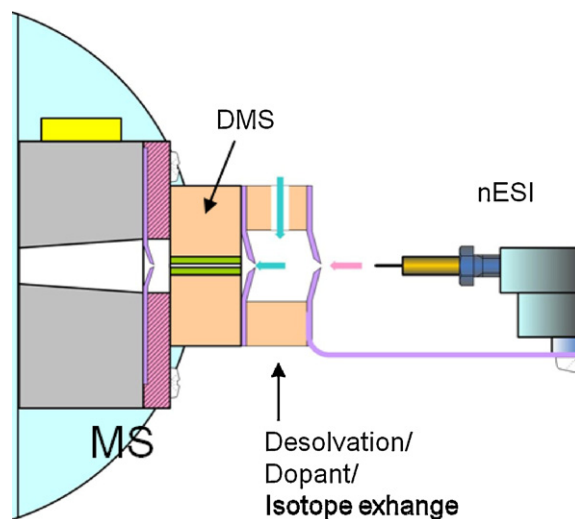


Fig. 1. Schematic of DMS/MS microspray interface. A Proxeon stainless steel nanospray emitter (nESI) is used, followed by a heated desolvation region, and a planar DMS section of 0.5 mm gap, 3 mm width and 10 mm length. Interface is shown as attached to a Waters ZQ, with inlet flow $600\text{ cm}^3/\text{min}$. The interface for the JEOL Accutof time-of-flight mass spectrometer is identical in design, with a JEOL-specific attachment in front of the inlet cone.

spectrometer operate independently, with DMS parameters controlled by serial interface and Sionex Expert 2.4.2 software, and the mass spectrometers by vendor software. A system fully integrating DMS parameters into the AB SCIEX Analyst hardware and software has been developed and is described in a separate publication [13]. The DMS high-frequency separation voltage (SV) and DC compensation voltage (CV) are provided by a half-cycle flyback-type generator that provides a clipped sinusoidal waveform (Sionex, Bedford, MA). SV operates at a fixed frequency of 1.25 MHz and covers a mean-to-peak amplitude range of 0–1500 V with CV capable of scanning at each SV over a range from -43 V to $+15\text{ V}$. In our sign convention, the applied field is of the form,

$$E(t) = E_S f(t) + E_C \quad (1)$$

where $f(t)$ is the unit-peak time dependence of the SV waveform, and E_S and E_C are the applied SV and CV voltages divided by the gap dimension. Optimal shape parameters for this type of waveform and methods of generation are considered in more detail in Krylov et al. [21].

For the Waters Micromass ZQ single-quadrupole system, the ions generated by the ion source are entrained in the transport gas flow of $600\text{ cm}^3/\text{min}$ generated by the mass spectrometer vacuum drag. The DMS voltage is applied transverse to the gas flow in an analytical region of dimension 0.5 mm (gap height) by 3.0 mm (width) by 10 mm (length). The micro-electrospray ion source used a Proxeon ES561 stainless steel emitter with flows of $300\text{ nL}/\text{min}$ and electrospray voltages of 1400 V unless otherwise stated. The temperature of the N_2 desolvation gas was maintained at 50°C with flows of approximately $100\text{ cm}^3/\text{min}$ unless otherwise stated. Although our newer integrated configurations on AB SCIEX instrumentation provide a counter-flow curtain gas that is highly effective in ensuring desolvation under higher liquid flows, the results reported here did not employ it. The importance of complete ion desolvation to eliminate widely heterogeneous cluster distributions for DMS operation is discussed in Schneider et al. [22]. In some cases, a drift-gas modifier was added to the desolvation gas using a headspace vapor delivery system as discussed in Refs. [14,15]. A more extensive discussion of the resolution enhancement due to drift-gas-modifier effects is provided in Schneider et al. [22,26]. For the JEOL Accutof time-of-flight system, the configuration was

similar, but additional nitrogen flow was introduced between the DMS filter and the mass spectrometer orifice to adjust the DMS transport flow from the 1100 cm³/min JEOL Accutof inlet flow to approximately 600 cm³/min, thereby maintaining DMS resolution [13]. The drift-gas modifier used was 1,2,3-trichloropropane, which provides enhancement of DMS resolution for anions similar to the more commonly used methylene chloride, but at lower concentration.

Samples were prepared in HPLC quality 50:50 methanol/water solutions from standards obtained from Sigma–Aldrich (USA or Canada) unless otherwise noted. The urine samples obtained from γ -irradiation mouse-model protocols [1,2,4], were diluted 1:4 with 50:50 acetonitrile/water, centrifuged, and further diluted 1:9 with an acetonitrile/methanol/water solvent (5:45:50) prior to analysis by electrospray at 300 nL/min. The samples were stored at –80 °C, except for 1 month after collection at –10 °C, as described in Tyburski et al. [1].

The data was analyzed both using instrument-specific software from JEOL (Mass Center v1.3.0n) and from Waters (MassLynx 4.0), and by an extensive set of custom MATLAB (Mathworks, Natick MA) applications. The MATLAB applications accessed the MS data in netCDF form using the SNCTOOLS/MEXNC interface [23]. The netCDF translations of native format MS data were generated by MS vendor software; JEOL Data Manager and Waters DataBridge, components of Mass Center and MassLynx, respectively.

3. Results and discussion

3.1. DMS–MS characteristics

A planar DMS–MS system for biomarker detection can provide performance advantages in selectivity and in sensitivity, as well as ease of use. These advantages include the following.

- Selectivity

1. *Separation of isobars.* Because DMS separation depends on ion properties that are largely independent of mass to charge ratio, DMS is able to separate isobaric compounds in many cases.
2. *Chemical noise reduction.* Electrospray ionization sources generate heterogeneous ion populations comprised of the ion of interest as well as a multitude of different ion species and clusters, as well as fragment ions generated in the source or in the atmosphere-to-vacuum interface. These ions are dispersed across the m/z range, contributing to chemical background. This chemical noise is usually greatly suppressed when DMS is tuned to select the target ion species for introduction into the MS.
3. *Separation of charge states.* Increasing charge both increases ion mobility, and, because collision energy is increased, changes the shape of the dependence of the curve describing mobility

on field. As a result, ion species occurring at the same m/z value but with different charge have much different DMS properties.

4. *Greater orthogonality than time-of-flight ion-mobility spectrometry (IMS).* DMS parameters are less correlated with mass than the IMS drift time [24,25] because DMS depends on additional non-geometric molecular properties such as charge distribution and polarizability, and because DMS accesses a range of effective temperatures during the DMS field cycle.

- Sensitivity

1. *Short residence time.* Residence times in planar DMS configurations are typically in the range of 1–4 ms. This short residence time reduces diffusion losses and minimizes unwanted reactions.
2. *Continuous operation.* DMS filtration, unlike time-of-flight IMS configurations, operates continuously without the ion losses caused by a shutter.
3. *Filtration of intact molecular ion.* MS/MS techniques are used to provide selectivity for many applications, but each fragmentation step in this method results in ion losses and the uncertainty in relative fragmentation efficiency requires careful calibration. DMS–MS operates on the ion prior to fragmentation while providing selectivity that can be equivalent to MS/MS. In addition, MS/MS techniques are time-consuming to apply in a mixture containing unknowns, because tentative identifications must be made and then verified in separate experiments. When necessary for confirmation of results, the DMS–CID–MS technique described in the section on isobar separation can provide verification of DMS ion selection based on the fragmentation pattern of a pre-selected ion population.

- Ease of use

1. *Transparent mode.* DMS in the planar configuration used here can be operated in transparent mode, which allows all ions to pass through the filter with minimum attenuation. This mode is used to optimize ion source operation. Differential mobility devices with cylindrical geometry do not have this capability.
2. *Constant intensity.* Planar DMS resolution is nearly independent of operating parameters separation voltage (SV) and compensation voltage (CV). The cylindrical or FAIMS configuration focuses or defocuses ions in a way that varies with separation voltage (SV) making intensities and resolution dependent on SV.
3. *Polarity independent.* Planar DMS operates to filter ions of both polarities, so no electrical changes are necessary when MS polarity is changed.

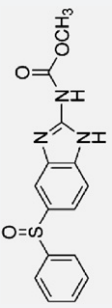
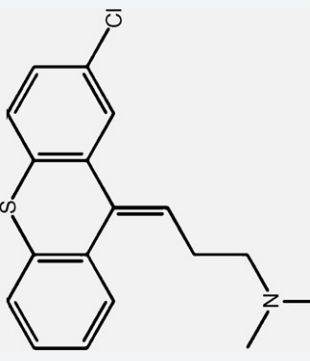
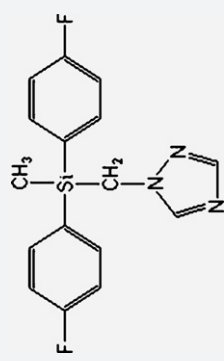
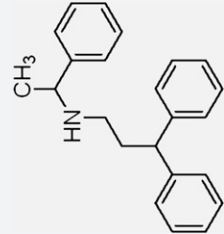
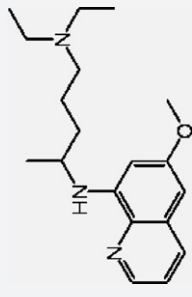
The following sections describe the DMS–MS experimental tests that have been performed to verify these expectations in the context of biomarker detection. We analyze DMS–MS performance for the separation of isobaric compounds, describing how DMS–MS with fragmentation at the MS inlet following DMS ion selection

Table 1

Five components of DMS–MS isobaric mixture. The five protonated molecules all were observed in mass spectrometry at 316 Da as shown in Fig. 2. The DMS ion filter resolves the mixture into 4 distinct peaks, with fendiline and chlorprothixene remaining partially resolved as shown in Figs. 2 and 3.

Chemical name (mass order)	Chemical formula	[M]/[MH] ⁺ mass/u	$\Delta m/u$	$R = 316 u/\Delta m$
Oxfendazole	C ₁₅ H ₁₃ N ₃ O ₃ S	315.06776 316.07559	0.01708	18,501
Chlorprothixene	C ₁₈ H ₁₈ ClNS	315.08484 316.09267	0.01549	20,400
Flusilazole	C ₁₆ H ₁₅ F ₂ N ₃ Si	315.10033 316.10815	0.09836	3212
Fendiline	C ₂₃ H ₂₅ N	315.19869 316.20652	0.03236	9765
Pamaquine	C ₁₉ H ₂₉ N ₃ O	315.23105 316.23889	–	–

Table 2
2D structures of the five compounds of Table 1.

Oxendazole	
Chlorprothixene	
Flusilazole	
Fendiline	
Pamaquine	

can operate in a mode like MS/MS of a triple-quadrupole instrument. We then examine separation of charge states, separation of biomarkers that are structural isomers, and give an example of DMS–MS applied to one of the urine samples used in biomarker discovery.

3.2. DMS–MS separation of isobaric compounds

The need to make quantitative measurements of multiple species occurring at nearly the same m/z or in the presence of isobaric interferences arising from chemical noise is one of the factors that drive the usage of very high resolution, and high cost, mass spectrometers. As a result, many diagnostic or analytical measurements cannot be made in field settings. If compounds close in m/z can be separated by DMS pre-filtration, high mass resolution is less important. In addition, quantification with triple-quadrupole MS/MS methods requires calibration based on product-ion scans of each target compound, while MS/MS sensitivity is reduced by loss of signal in the fragmentation step that is highly compound dependent.

As a reference point for isobaric separations, we have analyzed two different mixtures, one of five isobaric compounds of mass 315 Da, and a second group of six nearly isobaric compounds of mass 308–309 Da. The first group of five compounds all appear in positive mode ESI-MS at the same unit m/z . Tables 1 and 2 provide the chemical identity and structure of the five compounds, each of which has been measured in DMS–MS under low fragmentation conditions at m/z 316 (as the protonated molecules, $[MH]^+$). Table 1 also gives the exact mass for the compounds and protonated molecules, as well as the m/z difference between ions, and the resolution required to resolve them.

We recorded DMS–MS spectra of each of the compounds separately at several separation voltages in order to identify compensation voltage peak positions for each compound. In order to visualize the challenge presented by the mixture, Fig. 2(A) presents the mixture mass spectrum under conditions that minimize fragmentation with no DMS separation (DMS-transparent mode, SV = 0, CV = 0 which passes all ions), obtained on the single-quadrupole Waters Micromass ZQ. The mass spectrum consists of a single peak group with isotopic satellite peaks. If the observations are examined in detail (zoomed inset to the figure), we see that the mass spectrum could be incorrectly interpreted as arising from a single ion, not five chemically distinct ions, with an isotope distribution typical of organic compounds in this mass range. Fig. 2(B) shows the DMS compensation voltage (CV) tuning characteristics at SV 1400 V of MS ion count for the base peak, m/z 316 $[MH]^+$, and for the next two higher m/z values, indicating the distribution of isotopic masses. The carrier of each peak is identified based on the DMS CV characteristics of standard samples. Four separate peaks are observed for the five compounds, with fendiline and chlorprothixene remaining unresolved. Of the five compounds only chlorprothixene contains chlorine. The presence of chlorprothixene ($C_{18}H_{18}ClNS$) overlapped with fendiline in the CV = +2 V peak is evident from the high relative intensity of m/z 318 $[MH+2]^+$ due to ^{37}Cl . Absence of chlorine in the other 3 peaks is demonstrated by low m/z 318 intensity compared to the m/z 316 base peak and m/z 317 intensities for the other ions.

To activate the molecular ions, approximating MS/MS conditions with initial DMS selectivity, we increased the inlet cone voltage to induce fragmentation at the atmospheric-pressure to vacuum interface of the mass spectrometer after the DMS filter. We refer to this method as DMS–CID–MS (DMS collision-induced dissociation mass spectrometry). Both DMS–CID–MS and DMS–MS (no fragmentation) are two-dimensional separation techniques because a full or selected mass spectrum is recorded at each setting of DMS SV and CV tuning parameters. DMS–CID–MS fragment iden-

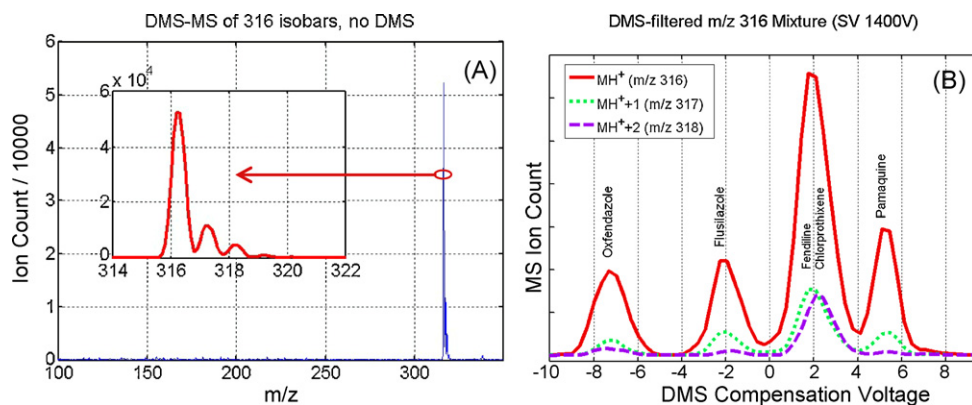


Fig. 2. (A) A single group of peaks appears at m/z 316 in nanoESI-MS of a mixture of the five compounds of Table 1 on Waters ZQ MS. DMS was operated in transparent mode (SV = 0, CV = 0) and the MS under non-fragmenting (low cone voltage) inlet conditions. Observed in DMS-transparent mode (0V SV, 0V CV) to transmit the entire ion population, $[MH]^+$ ions of m/z 316 appear as a single group of isotopic peaks. (B) When DMS separation voltage (SV) of 1400 V peak is applied, four DMS peaks are obtained for the five molecular ions, leaving chlorprothixene and fendiline unresolved. DMS peaks are identified by comparison with standards. The presence of chlorprothixene ($C_{18}H_{18}ClNS$) overlapped with fendiline in the CV = +2 V peak is evident from the high relative intensity of m/z 318 $[MH+2]^+$ due to ^{37}Cl . Absence of Cl in the other 3 peaks is demonstrated by low m/z 318 intensity compared to the m/z 316 base peak intensity for the other ions.

tifications are obtained by first DMS-selecting specific ion species and then passing them into the mass spectrometer with additional energy from the inlet cone voltage difference. This provides a level of specificity similar to a triple-quadrupole instrument. Fragments obtained in this way originate from the DMS-selected ion only, by may require some extra scrutiny because of possible ion reactions in the MS inlet area and DMS selectivity can be limited by overlapping features in DMS CV tuning.

Fig. 3(A) presents the DMS–CID–MS results for each of the five compounds in the five-component mixture obtained at SV 1200 V by using CV values of -6.15 V, -1.65 V, -0.08 V, $+2.22$ V, and 3.8 V for DMS selection of oxefendazole, flusilazole, fendiline, chlorprothixene, and pamaquine, respectively. To minimize effects from the overlap of fendiline and chlorprothixene DMS peak shapes, CV values at the edges of the feature were used. The “All Ions” trace was computed by summing mass spectra at all CV values recorded across the CV scan. Dominant fragments selected from these results allow us to use fragment MS spectra to evaluate in another way the selectivity achieved by DMS. Table 3 shows peak positions observed for separation voltages of 1200 V (106 Td at 1 atm, $50^\circ C$), and 1400 V (123 Td). DMS compensation voltages for these compounds with SV 1200 V span approximately 10 V, with peak widths of 1.2–1.5 V. In Fig. 3(B), using the characteristic fragment ions in the table, each of the five ions is separately detected. Fendiline and chlorprothixene are overlapped, as expected from the

previous figure. All ions are resolved, but signal intensities detected through the CID fragment spectrum for these five compounds are typically 30% of the signals observed using DMS–MS for the same species.

We have also tested DMS–MS performance on a set of six compounds of approximately the same mass. These six compounds, benoxinate, bestatin, nifenazone, phenylbutazone, quinoxifen, and warfarin have molecular weights of 308 Da, except for quinoxifen at 307 Da. All formulas, structure, and computed isotope ratios for the ion species related to this mixture are given in the supplemental material for this paper. Fig. 4 shows the DMS–MS analysis at characteristic m/z values for the base peaks and isotopes, similar to Fig. 2(B), of nanoESI of the 6-component mixture. Conditions minimizing fragmentation at the DMS–MS transition were used so that the MS contained only $[MH]^+$ and $[MNa]^+$ base peaks, maximizing sensitivity. The $[MH]^+$ base peak of quinoxifen is m/z 308 and $[MH]^+$ is m/z 309 for bestatin, benoxinate, nifenazone, and phenylbutazone. The mass spectrum near m/z 309 without DMS separation is shown in the inset to the figure. $[warfarin-Na]^+$ and $[phenylbutazone Na]^+$ were also observed and appear at m/z 331, as labeled. All but one pair of ions (benoxinate, nifenazone) are resolved by the combined DMS–MS performance (DMS alone at m/z 331 for warfarin Na^+ and phenylbutazone Na^+ , and at m/z 308–9 for protonated quinoxifen, bestatin and phenylbutazone). Benoxinate and nifenazone remain unresolved at 1400 V. They are

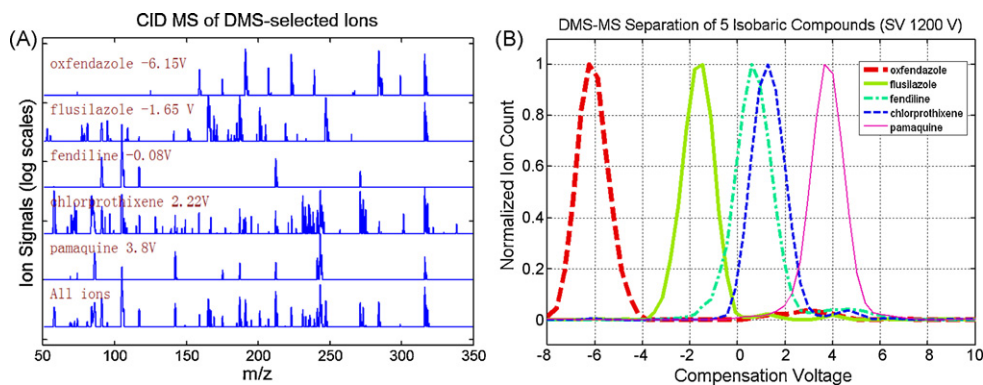


Fig. 3. (A) Setting a high inlet cone voltage allows characteristic fragment ions for each of the five molecular ions to be identified, at a cost of reduced sensitivity due to the multiple fragmentation paths for each of the ions. SV 1200 V was used with CV values of -6.15 V, -1.65 V, -0.08 V, $+2.22$ V, and 3.8 V DMS selection of oxefendazole, flusilazole, fendiline, chlorprothixene, and pamaquine, respectively. To minimize effects from the overlap of fendiline and chlorprothixene, CV values at the edges of the feature were used. The All Ions trace was computed by summing mass spectra at all CV values. (B) DMS–MS separation of the five isobaric compounds (Table 1) at SV = 1200 V visualized based on fragments selected for each ion from panel (A) of this figure. The specific fragment ions are listed in Table 3.

Table 3

DMS–MS characteristics of the isobaric mixture of five compounds. Results are given for DMS separation voltages (SV) of 1200 V (106 Td) and 1400 V (123 Td), positive MS ion mode. MS/MS information was determined by inducing CID in the inlet cone. The fragment peaks listed in parentheses were chosen from among the dominant fragments for each compound, to provide the DMS separation shown in Fig. 3(B). Compensation voltage (peak positions), peak widths, and separation from the next peak are shown for SV 1200 V and SV 1400 V. Except for fenflinane and chlorprothixene, all compounds are fully resolved by DMS alone. Compensation voltage, peak width, and separation between adjacent peaks (ΔCV) are in volts.

Compound (CID/MS ion m/z)	Compensation voltage (1200 V/1400 V)	Peak width (1200 V/1400 V)	CV spacing to next peak (1200 V/1400 V)
Oxfendazole (191.2)	−6.2/−7.0	1.2/2.4	4.4/5.5
Flusilazole (165.2)	−1.8/−1.5	1.3/1.4	2.2/3.5
Fenflinane (105.1, 91.1, 212.3)	0.4/2.0	1.2/1.9	0.6/0.8
Chlorprothixene (271.2, 84.1)	1.0/2.8	1.5/1.7	2.5/2.9
Pamaquine (243.3)	3.5/5.7	1.4/1.6	–

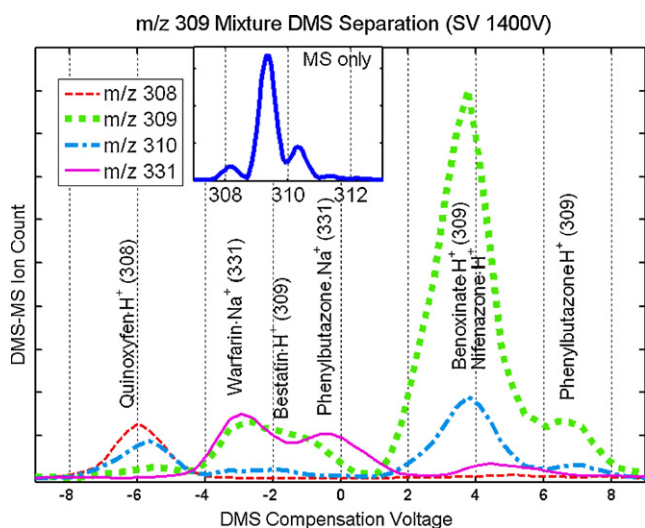


Fig. 4. NanoESI-DMS–MS 2D spectrum of the six component mixture is shown for SV 1400 V. At each DMS compensation voltage, a full mass spectrum was obtained, but MS ion counts are shown only for characteristic masses. All but one pair of ions (benoxinate, nifenazone) are resolved by the combined DMS–MS performance (DMS alone at m/z 331 for warfarin Na^+ and phenylbutazone Na^+ , and at m/z 308–9 for quinoxifen, bestatin and phenylbutazone). Benoxinate and nifenazone remain unresolved at 1400 V. They are partially separated by 1 V CV at SV 1200 V (peak FWHM ~ 1.6 V), but other separations are reduced.

partially separated by 1 V CV at SV 1200 V (peak FWHM ~ 1.6 V) but separation of the other ions is reduced at the lower separation voltage.

For the six compound mixture, characteristic fragment ions could not easily be identified by DMS–CID–MS to distinguish each compound from all others. Because DMS separation is based on the ion before fragmentation, it is not ambiguous in this way, but peak

positions must be identified by the use of standards, as was done to determine the labels in Fig. 4. In this mixture, quinoxifen contains two chlorine atoms, resulting in a very different pattern of intensities of isotopic peaks from other components of the mixture. This makes it possible to test the quality of the quinoxifen separation by measuring isotope ratios. The observed and predicted isotopic peak intensities for [quinoxifen-H] $^+$ and for [phenylbutazone-H] $^+$ are shown in Fig. 5, and the agreement with predictions is good.

DMS is especially useful in combination with mass spectrometry because its separation mechanism is complementary to m/z . The presented examples show how useful DMS can be in resolving mixtures that are difficult for mass spectrometry, in this case without the use of clustering modifiers in the DMS transport gas. The use of polar modifiers in the drift-gas results in 8–10-fold improvement in DMS resolution, as discussed in more detail below for the citrate–isocitrate separation, and in Schneider et al. [26].

3.3. DMS separation of charge states

In complex samples ionized in atmospheric pressure sources, ions may be created with more than one charge state. Heavier ions that are multiply charged by the ion source appear in the same m/z range as lighter species. For small molecule biomarkers, this aliasing of heavier species into the m/z range of the biomarker causes errors in intensities, and adds complexity to the mass spectrum. This resulting degradation of the mass spectrum is similar in effect to the interference from chemical noise that is generated when heavy ions fragment into lighter ions in the biomarker range. Both effects can be reduced by a DMS prefilter. Multiply-charged ions typically have compensation voltages that are more positive than singly charged ions with the same m/z . Two effects are involved in this result: (1) multiply-charged ions are field-accelerated more strongly, so the hard-collision limit is reached more rapidly, and

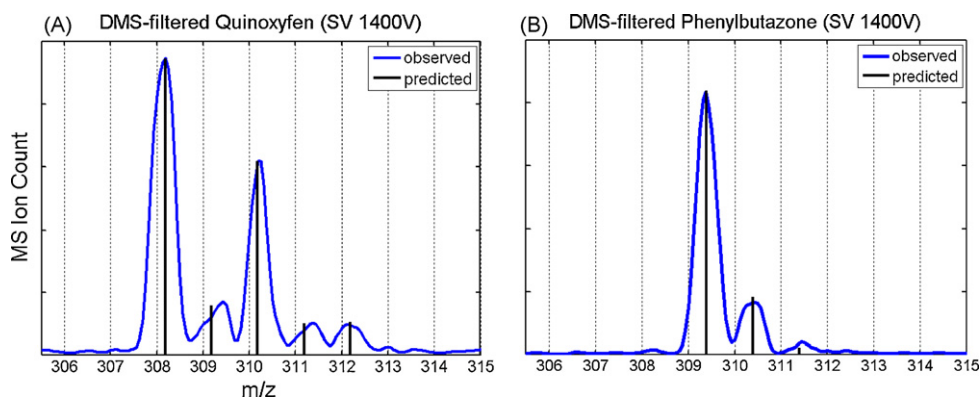


Fig. 5. (A) Quinoxifen ($\text{C}_{15}\text{H}_8\text{Cl}_2\text{FNO}$) is here selected as $[\text{MH}]^+$ by CV -6 V for SV 1400 V. The observed DMS-selected mass spectrum is shown and compared with predicted isotopic ratios. (B) Phenylbutazone ($\text{C}_{19}\text{H}_{20}\text{N}_2\text{O}_2$) is selected as $[\text{MH}]^+$ by CV $+7$ V for SV 1400 V. The observed DMS-selected mass spectrum is shown and compared with predictions. Both agree well, but only the quinoxifen pattern is greatly different from predictions for the other components of the mixture, due to the presence of chlorine.

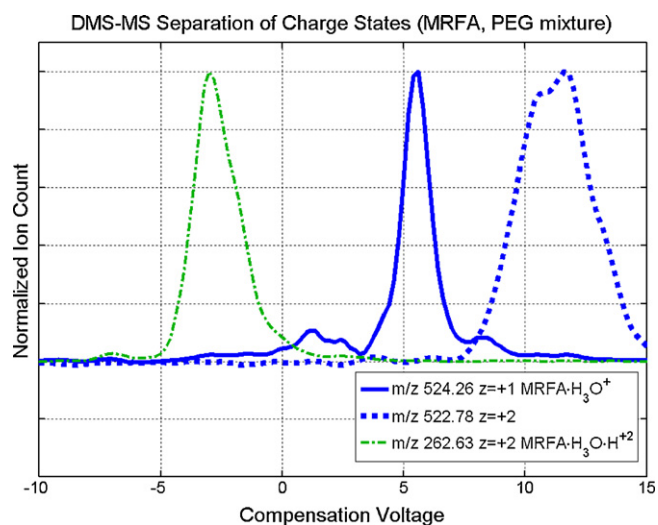


Fig. 6. DMS–MS spectra of MRFA/PEG mixture for selected m/z values showing DMS separation by charge state. The tetrapeptide MRFA was mixed with polyethylene glycols (200–800 Da) and recorded on a JEOL Accutof TOF in positive ion mode. Ions of nearly the same m/z and of nearly the same mass are shown. DMS resolves $[\text{MRFA}\cdot\text{H}_3\text{O}]^+$ at m/z 524.2 from a doubly charged species at m/z 522.7 and a doubly charged MRFA species ($[\text{MRFA}\cdot\text{H}_3\text{O}\cdot\text{H}]^{2+}$) at m/z 262.63.

(2) larger ions often have internal van der Waals interactions that reduce the strength of interactions with the drift gas, making ion-neutral interactions more hard-sphere-like [22,26]. In addition, ions within chemical series also tend to move to positive CV as mass increases, but for similar m/z values the separation between charge states is large.

With DMS, we frequently observe a reduction in chemical noise, in which interfering mass peaks are suppressed and correct isotope ratios are restored for a particular target species. For this particular example, we have observed DMS separation of two charge states that occur at similar m/z values. The sample was a mixture of the tetrapeptide methionine-arginine-phenylalanine-alanine (MRFA) and polyethylene glycols (PEG) from 400 Da to 600 Da, in 50/50 methanol/water. Fig. 6 shows DMS resolution of $[\text{MRFA}\cdot\text{H}_3\text{O}]^+$ at m/z 524.2 from a doubly charged species at m/z 522.7 and from a doubly charged ion of lower m/z , on a JEOL Accutof TOF. The complete mass spectrum is not shown, but is complicated with many near coincidences and contains a variety of MRFA/PEG clusters and fragments. The two species that are nearly coincident in mass to charge ratio ($z=+1$, $m/z=524.2$ $[\text{MRFA}\cdot\text{H}_3\text{O}]^+$, and $z=+2$, m/z 522.7 (PEG related)) are separated by +6.2 V in DMS compensation voltage. It is of less practical importance for DMS–MS applications because the species are separated by low-resolution mass spectrometry alone, but Fig. 6 also shows DMS–MS characteristics for the doubly charged species $[\text{MRFA}\cdot\text{H}_3\text{O}\cdot\text{H}]^{2+}$, which is separated by an additional 8.5 V from the singly charged species. For the nearly coincident peaks near m/z 524, DMS is able to select either species, completely suppressing the other. In Fig. 7, DMS-filtered mass spectra in the range from m/z 520 to 530 for the MRFA/PEG mixture are shown at the compensation voltages that select each peak (1200 V SV): +5.6 V in the upper panel, selecting $[\text{MRFA}\cdot\text{H}_3\text{O}]^+$, and +11.8 V in the lower panel selecting the doubly charged species. Both doubly charged and singly charged ions, within chemical series tend to move to positive CV as mass increases, but for similar m/z values the separation between charge states is large, with the higher charge state to more positive CV. These specific CV values depend on the concentration of neutral solvent modifier molecules in the transport gas stream, but are stable under standardized conditions, as we have discussed in other publications [22,26].

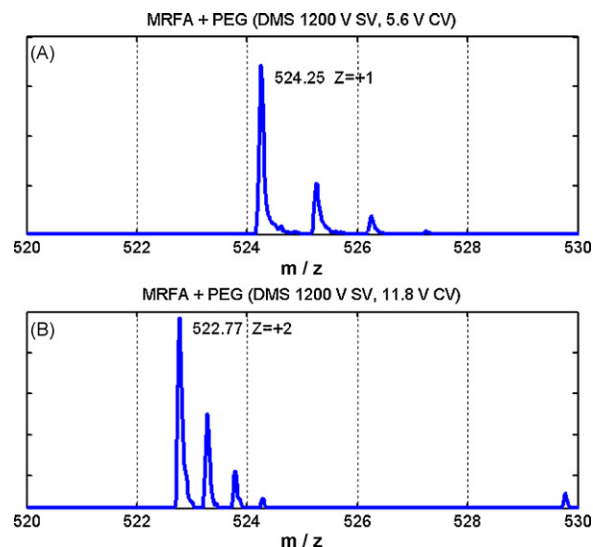


Fig. 7. DMS-filtered mass spectrum from m/z 520 to 530 for the MRFA/PEG mixture. The compensation voltage for the doubly charged species is +6.2 V higher than that of the singly charged $[\text{MRFA}\cdot\text{H}_3\text{O}]^+$ ion of similar m/z . Within a charge state, higher mass species occur at more positive compensation voltage. See text for further discussion.

3.4. DMS–MS separation of candidate biomarkers citrate/isocitrate

Citrate and/or isocitrate have been identified as potential biomarkers both by the LC–MS studies [1] and the GC–MS study [3] using classification techniques such as orthogonal partial least squares and random forests, and are associated with some of the largest metabolomic signals. Citric acid and isocitric acid are important in the citric acid cycle, in glycolysis, and in cellular respiration. Citric acid is achiral, but isocitric acid can have both D and L forms. Our sample of citric acid was the citric acid monohydrate while isocitrate was obtained as the tri-sodium salt of DL-isocitric acid.

Because these two compounds are structural isomers, with identical chemical compositions, both appear in the anion mass spectrum at m/z 191, as $[\text{M}-\text{H}]^-$. Nonetheless, at high separation voltages, we find that the citrate and isocitrate ions appear to be weakly separated by DMS under the conditions used here. This separation cannot be achieved by mass spectrometry, or by low field ion-mobility techniques. This result is shown in Fig. 8(A). The citrate and isocitrate samples were prepared identically and run sequentially. Nonetheless, this weak separation would be expected to have some dependence on spray conditions and this small separation would not be reliable in production analytical applications. A modification to the technique which would increase the separation is necessary for applications, and we find that use of a transport gas modifier is effective.

DMS resolution can be improved by additions known as modifiers to the composition of the transport gas used to carry ions through the DMS into the mass spectrometer. This is a technique that is applicable to essentially all systems, but is especially useful when chemical and structural differences are small [22,26,14,15]. The choice of modifier depends on ion polarity and, to a lesser degree, on the chemical structure of the target ions. These modifiers participate in field-dependent clustering and declustering in the DMS separation field, increasing the difference between high and low field mobilities, thereby increasing the compensation voltage. For negative ions, chloride-based modifiers are frequently effective. By adding a small partially chlorinated aliphatic hydrocarbon (~0.1% 1,2,3-trichloropropane in this case) to the desolvation gas, we have found that citrate can be detected separately from isoc-

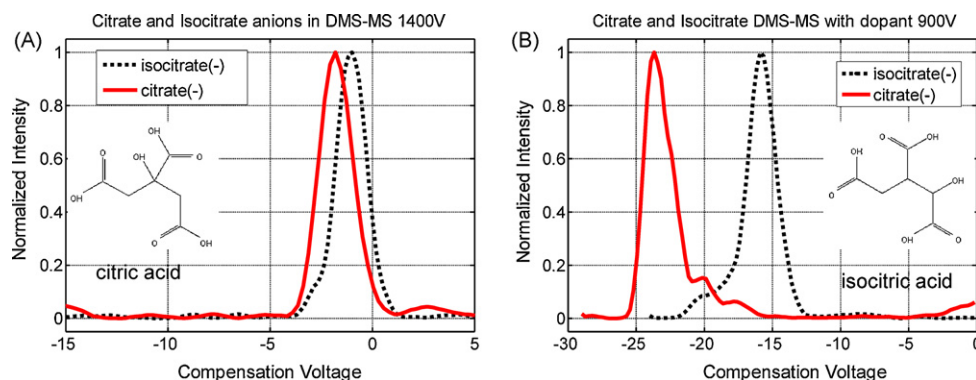


Fig. 8. (A) DMS–MS of citrate and isocitrate anions. These two isobaric ions are weakly separated by DMS with no modifier in the transport gas at 1400 V SV under these conditions. (B) DMS–MS of citrate and isocitrate anions with drift-gas modifier. Citrate and isocitrate can be fully separated by DMS with the addition of chloride-type modifiers in the transport gas. In this case, 1,2,3-trichloropropane was used as the modifier, but chlorine-containing organics such as methylene chloride are also effective. The structures of citric acid and isocitric acid are included for convenience of the reader.

itrate, as shown in Fig. 8(B). Chlorine-containing modifiers have been used for some time in a number of contexts such as explosives detection [27], to enhance DMS separation of anions and are believed to be mediated by chloride anion.

The use of drift-gas modifiers to enhance separation for cations and for anions in planar DMS instrumentation is an active area of investigation and has recently been shown to lead to an order of magnitude increase in selectivity when evaluated over a wide spectrum of target ions in for complex mixtures [26]. The enhanced citrate–isocitrate separation shown here is another example of the general utility of the technique.

3.5. DMS–MS separation of dicarboxylic acids

The most recent radiation biomarker paper [3] identifies several aliphatic dicarboxylic acids as down-regulated biomarkers (adipic, pimelic, suberic, azelaic acids ($\text{HO}_2\text{C}-(\text{CH}_2)_j-\text{CO}_2\text{H}$), for $j = 4-7$). The dicarboxylic acids appear as anions with negative compensation voltages, near -10 V CV for 1000 V SV (88 Td). This characteristic distinguishes them from many of the other biomarkers, and from typical interferences. In addition, these ions are detected with high sensitivity under low-CID conditions. In analyzing a standard, we found that the azelaic acid sample contained traces of other dicarboxylic acids, with $j = 5-10$, and provided an interesting demonstration of DMS separation of a related series of compounds. Fig. 9 shows DMS separation of dicarboxylic acids appearing in azelaic acid sample obtained for 1000 V SV . The acids are $\text{HO}_2\text{C}(\text{CH}_2)_j\text{CO}_2^-$ for $j = 5-10$ ($j = 5$ (pimelic acid), $j = 6$ (suberic acid), $j = 7$ (azelaic acid), $j = 8$ (sebacic acid), $j = 9$ (undecanedioic acid) and $j = 10$ (dodecanedioic acid)) appearing as the deprotonated molecules. Each of the DMS peaks is separated by 1 V or more in compensation voltage. The curve peaking at -10 V under the conditions of Fig. 9 is azelaic acid. Shorter chain acids appear at more negative compensation voltages, longer chains at more positive values. In Fig. 9, the peaks are labeled by relative intensities of the separate ion signals in the DMS-transparent and DMS-filtered mass spectra, and show a dynamic range of approximately 500.

3.6. DMS–MS testing on bio-fluid samples

Radiation-exposure biomarker discovery by high-resolution ultra-performance liquid chromatography time-of-flight mass spectrometry (UPLC–TOFMS) described in the first two of the recent group of papers is based on a comparison of urine samples from exposed and sham-treated mice, with doses ranging from 0 to 8 Gy [28]. Both of these studies identified *N*-hexanoylglycine as a relevant biomarker, along with a number of other candidate or

validated biomarkers. The most recent study [3], based on a rat model, uses chemical derivatization followed by GC–MS, did not identify this compound, which may be unstable under these conditions, but does have a number of other biomarker identifications in common with the LC–MS work. As an example of the performance of DMS–MS on biological samples, we examine the DMS–MS negative ion spectrum using the single-quadrupole Waters ZQ of a urine sample from the treated group in the mass range that includes both *N*-hexanoylglycine, and suberic acid. These molecules are identified as biomarkers by LC–MS and GC–MS studies, respectively.

Suberic acid DMS–MS properties in negative ion mode are shown in Fig. 9 along with those of several other dicarboxylic acids, for nanospray from methanol/water solution. *N*-Hexanoylglycine also appears most strongly in negative ion mode. In the medical and scientific literature, *N*-hexanoylglycine is associated with medium-chain acyl-coA dehydrogenase deficiency (MCAD, Reyes syndrome), with dicarboxylic aciduria [29], and with a few other conditions [30]. This compound has also been the subject of previous GC–MS studies in a medical context [31].

The DMS–MS results for the urine sample from the treated group are shown in Fig. 10 under three different conditions: no DMS selectivity (inset), DMS-selecting *N*-hexanoylglycine, and DMS-selecting

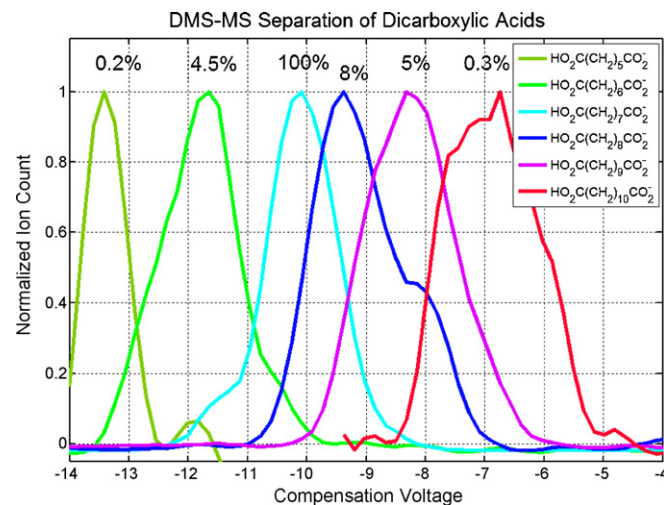


Fig. 9. DMS separation of dicarboxylic acids appearing in azelaic acid sample. In the legend, from top to bottom, and left to right in the figure, are $\text{HO}_2\text{C}(\text{CH}_2)_j\text{CO}_2^-$ for $j = 5-10$ ($j = 5$ (pimelic acid), $j = 6$ (suberic acid), $j = 7$ (azelaic acid), $j = 8$ (sebacic acid), $j = 9$ (undecanedioic acid) and $j = 10$ (dodecanedioic acid)), each separated by 1 V or more in compensation voltage. The curve peaking at -10 V is azelaic acid. Separation voltage (SV) was 1000 V .

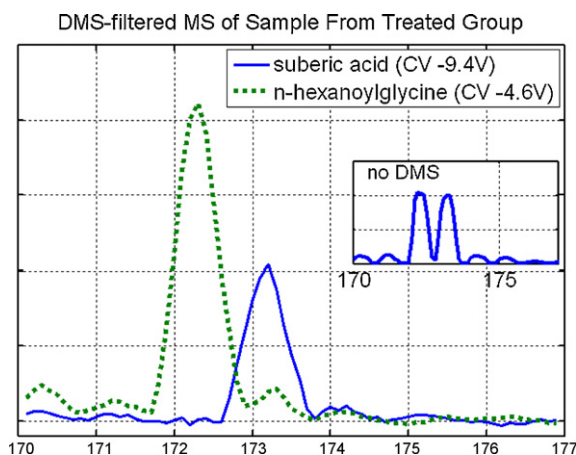


Fig. 10. DMS–MS mass spectrum of mouse urine from treated group at SV 1000 V, resolving 2 biomarkers from each other, and suppressing a background of chemical noise. The peak at m/z 172 (CV -4.6 V) was identified as *N*-hexanoylglycine by comparing fragmentation of the DMS-filtered ion from the biosample to the DMS-filtered fragmentation of a standard. The peak at m/z 173 has DMS properties consistent with suberic acid, $\text{HO}_2\text{C}(\text{CH}_2)_6\text{CO}_2^-$, m/z 173, and presents the expected isotope ratios but this peak was not similarly texted for fragmentation properties. The inset figure shows the spectrum in this range without DMS filtration (600 V SV, summed over all CV values).

suberic acid. $[\text{M}-\text{H}]^-$ signals for *N*-hexanoylglycine and suberic acid appear at m/z 172 and 173, respectively.

Without DMS selectivity, each peak intensity is due to some intensity from the desired peaks, but also includes additional intensity from main and isotope peaks of compounds nearby or identical in mass and fragments and clusters originating from other compounds in the complex matrix, which are transformed into the biomarker mass range either in the ionization process or in the mass spectrometer interface. Quantitative measurement is difficult under these conditions, especially for low concentrations.

With DMS, these interferences are suppressed and the spectra at m/z 172 and 173 are observed separately, at distinct DMS compensation voltages. The identity of hexanoylglycine in the DMS-filtered mass spectrum was verified by observing identical fragmentation patterns of the DMS-selected mass peak in the biosample in comparison with that of a pure standard, and by comparison of the DMS compensation voltage from a standard. Suberic acid was not verified by MS/MS in this series of tests, but the DMS compensation voltage is in agreement with the value from a standard. In addition, the intensity of the $[\text{M}+1]$ isotope peak for the separated compounds is in agreement with the predicted $[\text{M}+1]/[\text{M}]$ ratio within 1%. Because it is possible to verify that selected intensity observed from the urine sample is due to the target biomarker, the measurement accuracy is improved, especially for biomarkers that appear at low concentrations where they may be completely lost in chemical noise. To perform the same analysis without DMS necessitates very high resolution, and/or MS/MS, and some other pre-separation techniques like LC or derivitization/GC.

Sensitivity and selectivity of DMS–MS is clearly adequate for these two biomarkers. For other biomarkers, the sensitivity depends on concentrations and is reduced by ion suppression effects that occur in a complex matrix [32]. Concentrations of the biomarker components in urine samples have been given as part of the biomarker discovery reports for only a few of the identified species. Tyburski et al. [1] list the concentrations relative to creatinine (typ. 3 mM) of *N*-hexanoylglycine as 400 $\mu\text{M}/\text{mM}$, of taurine as 8 mM/mM, and of β -thymidine as 6–10 $\mu\text{M}/\text{mM}$. Even considering suppression effects, the concentrations of *N*-hexanoylglycine and taurine are readily detectable, and are quantifiable by controlled addition. β -Thymidine has not yet been detected in our DMS–MS

testing of biofluids. Thymidine is subject to significant suppression effects, occurs at a low concentration, and has not always been detected in animal model testing. Quantitative measurements of concentrations for other biomarkers would be useful, but is not currently available.

4. Conclusion

The results given in this paper provide representative DMS–MS experimental results that test system performance in the context of biomarker detection. DMS–MS is effective in suppressing chemical noise and separating interfering ions in chemical mixtures containing several ions of similar molecular weight and mass to charge ratio, and in complex biological samples. We have presented a wide range of results relevant to instrumentation for metabolomic small-molecule radiation-exposure biomarkers. These controlled experimental results have included the separation of isobars, the separation of charge states, the separation of biomarker candidates citrate and isocitrate, and the separation of a series of dicarboxylic acids.

For the bio-fluid sample, we have also demonstrated suppression of chemical noise and separation of near-isobars. From both sensitivity and selectivity points of view, as discussed in the previous section, DMS–MS appears to be effective for direct analysis of some identified biomarkers in biosamples with minimal sample preparation.

Additional testing and development is necessary before it becomes possible to apply rapid DMS–MS in field conditions as an alternative to lab processing with UPLC–TOFMS or similar time-consuming and expensive techniques. Nonetheless, DMS–MS promises to be rapid and powerful for radiation exposure and possibly other biomarker screening applications. We believe that DMS–MS allows the development of field-portable devices based on mass spectrometers of moderate resolution that will obtain results equivalent to more sophisticated lab-based instrumentation. A field-portable DMS–MS system would automate the preparation and processing of bio-fluid samples to determine concentration relative to an internal reference (e.g., creatinine) of a few metabolomic biomarkers for radiation exposure. Based on the on-going discovery efforts and additional analysis of experimental data to determine the statistical validity of multiple simultaneously determined biomarker concentrations, a DMS–MS instrument of the proposed type would be able to identify cases of radiation exposure at levels requiring therapeutic intervention.

Acknowledgements

This work was supported by the Columbia University Center for Medical Countermeasures against Radiation (Principal Investigator Prof. David Brenner), and funded by NIH/NIAID grant U19 AI067773-02. We would especially like to thank Jeffrey R. Idle for support of Sionex participation in this project and for his contribution to the identification of the biomarkers described in Refs. [1–4].

Appendix A. Supplementary data

Supplementary data associated with this article can be found, in the online version, at doi:10.1016/j.ijms.2010.01.013.

References

- [1] J.B. Tyburski, A.D. Patterson, K.W. Krausz, J. Slavik, A.J. Fornace, F.J. Gonzalez, J.R. Idle, Radiation metabolomics. 1. Identification of minimally invasive urine biomarkers for gamma-radiation exposure in mice, *Radiat. Res.* 170 (2008) 1–14.

- [2] A.D. Patterson, H. Li, G.S. Eichler, K.W. Krausz, J.N. Weinstein, A.J. Fornace, F.J. Gonzalez, J.R. Idle, UPLC-ESI-TOFMS-based metabolomics and gene expression dynamics inspector self-organizing metabolomic maps as tools for understanding the cellular response to ionizing radiation, *Anal. Chem.* 80 (2008) 665–674.
- [3] C. Lanz, A.D. Patterson, J. Slavík, K.W. Krausz, M. Ledermann, F.J. Gonzalez, J.R. Idle, Radiation metabolomics. 3. Biomarker discovery in the urine of gamma-irradiated rats using a simplified metabolomics protocol of gas chromatography-mass spectrometry combined with random forests machine learning algorithm, *Radiat. Res.* 172 (2009) 198–212.
- [4] J.B. Tyburski, A.D. Patterson, K.W. Krausz, J. Slavík, A.J. Fornace, F.J. Gonzalez, J.R. Idle, Radiation metabolomics. 2. Dose- and time-dependent urinary excretion of deaminated purines and pyrimidines after sublethal gamma-radiation exposure in mice, *Radiat. Res.* 172 (2009) 42–57.
- [5] T.C. Pellmar, S. Rockwell, Priority list of research areas for radiological nuclear threat countermeasures, *Radiat. Res.* 163 (2005) 115–123.
- [6] “Every senior leader, when you’re asked what keeps you awake at night, it’s the thought of a terrorist ending up with a weapon of mass destruction, especially nuclear.” U.S. Secretary of Defense R. Gates in B. Graham, et al., *The Report of the Commission on the Prevention of WMD Proliferation and Terrorism*, Vintage Books, New York, 2008.
- [7] I.A. Buryakov, E.V. Krylov, A.L. Makas, E.G. Nazarov, V.V. Pervukhin, U.Kh. Rasulev, Drift spectrometer for the control of amine traces in the atmosphere, *Zhurnal Analiticheskoi Khimii* 48 (2) (1993) 114–121.
- [8] G.A. Eiceman, Z. Karpas, *Ion Mobility Spectrometry*, second edition, CRC Press, 2005, ISBN: 9780849322471.
- [9] R. Guevremont, High-field asymmetric waveform ion mobility spectrometry: a new tool for mass spectrometry, *J. Chromatogr. A* 1058 (1–2) (2004) 3–19.
- [10] R. Guevremont, B. Makowski, Using FAIMS to increase selectivity for LC–MS analyses, *Am. Lab.* 37 (13) (2005) 11.
- [11] M.A. McCooeye, Z. Mester, B. Ells, D.A. Barnett, R.W. Purves, R. Guevremont, Quantitation of amphetamine, methamphetamine, and their methylenedioxy derivatives in urine by solid-phase microextraction coupled with electrospray ionization-high-field asymmetric waveform ion mobility spectrometry-mass spectrometry, *Anal. Chem.* 74 (13) (2002) 3071–3075.
- [12] A.A. Shvartsburg, *Differential Ion Mobility: Non-Linear Ion Transport and Fundamentals of FAIMS*, CRC Press, Taylor and Francis LLC, Boca Raton, FL, 2008.
- [13] B.B. Schneider, T.R. Covey, S.L. Coy, E.V. Krylov, E.G. Nazarov, Planar differential mobility spectrometer as a pre-filter for atmospheric pressure ionization mass spectrometry, *Int. J. Mass Spectrom.*, in press (and references therein).
- [14] D.S. Levin, R.A. Miller, E.G. Nazarov, P. Vouros, Rapid separation and quantitative analysis of peptides using a new nanoelectrospray-differential mobility spectrometer-mass spectrometer system, *Anal. Chem.* 78 (2006) 5443.
- [15] D.S. Levin, P. Vouros, R.A. Miller, E.G. Nazarov, Using a nanoelectrospray-differential mobility spectrometer-mass spectrometer system for the analysis of oligosaccharides with solvent selected control over ESI aggregate ion formation, *J. Am. Soc. Mass Spectrom.* 18 (2007) 502.
- [16] B.M. Lolakowski, Z. Mester, Review of applications of high-field asymmetric waveform ion mobility spectrometry (FAIMS) and differential mobility spectrometry (DMS), *Analyst* 132 (2007) 842–864.
- [17] The Sionex microAnalyzer, for instance, is a self-contained trap/GC system with DMS detection that provides ppb/ppt sensitivity (<http://www.sionex.com>).
- [18] S. Kandler, G.R. Lambertus, B.D. Dunietz, S.L. Coy, E.G. Nazarov, R.A. Miller, R.D. Sacks, Fragmentation pathways and mechanisms of aromatic compounds in atmospheric pressure studied by GC–DMS and DMS–MS, *Int. J. Mass Spectrom.* 263 (2007) 137.
- [19] E.G. Nazarov, R.A. Miller, G.A. Eiceman, J.A. Stone, Miniature differential mobility spectrometry using atmospheric pressure photoionization, *Anal. Chem.* 78 (2006) 4553–4563.
- [20] Patent application (WO/2008/085357), (PCT/US2007/025929), Surface Enhanced Raman Spectroscopy Detection With Ion Separation Pre-Filter.
- [21] E.V. Krylov, S.L. Coy, E.G. Nazarov, J. Vandermeij, B.B. Schneider, T.R. Covey, *Rev. Sci. Instrum.* 81 (2010) 024101.
- [22] B.B. Schneider, T.R. Covey, S.L. Coy, E.V. Krylov, E.G. Nazarov, Control of chemical effects in the separation process of a differential mobility/mass spectrometer system, *Eur. J. Mass Spectrom.* 16 (1) (2010) 57–71.
- [23] <http://mexcdf.sourceforge.net/> provides access to the SNCTOOLS/MEXNC MATLAB interface to netCDF format files. The SNCTOOLS/MEXNC interface is being superceded by native MATLAB support for netCDF files, beginning with MATLAB R2008b.
- [24] A.A. Shvartsburg, K. Tang, R.D. Smith, Two-dimensional ion mobility analyses of proteins and peptide, *Methods Mol. Biol.* 492 (2009), doi:10.1007/978-1-59745-493-3_26.
- [25] P. Dwivedi, P. Wu, S.J. Klopsch, G.J. Puzon, L. Xun, H.H. Hill, Metabolic profiling by ion mobility mass spectrometry (IMMS), *Metabolomics* 4 (2008) 63–80, doi:10.1007/s11306-007-0093-z.
- [26] B.B. Schneider, T.R. Covey, S.L. Coy, E.V. Krylov, E.G. Nazarov, Chemical effects in the separation process of a differential mobility/mass spectrometer system, *Anal. Chem.*, doi:10.1021/ac902571u, in press.
- [27] G.A. Eiceman, E.V. Krylov, N.S. Krylova, E.G. Nazarov, R.A. Miller, Separation of ions from explosives in differential mobility spectrometry by vapor-modified drift gas, *Anal. Chem.* 76 (2004) 4937–4944.
- [28] Gray, abbreviated Gy, 1 J of energy absorbed per kilogram of tissue.
- [29] C.R. Roe, D.S. Millington, D.A. Maltby, T.P. Bohan, S.G. Kahler, R.A. Chalmers, Diagnostic and therapeutic implications of medium-chain acylcarnitines in the medium-chain acyl-coA dehydrogenase deficiency, *Pediatr. Res.* 19 (5) (1985) 459–466.
- [30] B.H. Baretz, H.S. Ramsdell, K. Tanaka, Identification of n-hexanoylglycine in urines from two patients with Jamaican vomiting sickness, *Clin. Chim. Acta* 73 (1) (1976) 199–202.
- [31] P. Rinaldo, J.J. O’Shea, R.D. Welch, K. Tanaka, Stable isotope dilution analysis of n-hexanoylglycine, 3-phenylpropionylglycine and suberylglycine in human urine using chemical ionization gas chromatography/mass spectrometry selected ion monitoring, *Biomed. Environ. Mass Spectrom.* 18 (7) (1989) 471–477.
- [32] R. King, R. Bonfiglio, C. Fernandez-Metzler, C. Miller-Stein, T. Olah, Mechanistic investigation of ionization suppression in electrospray ionization, *J. Am. Chem. Soc.* 111 (2000) 942–950.